RESEARCH STRATEGY

BACKGROUND and SIGNIFICANCE

Thiamine is a critical enzyme cofactor within the glycolytic metabolism network that is fundamentally required to sustain the bioenergetic and anabolic needs of all cells. Thiamine or more specifically the activated cofactor, thiamine diphosphate (TDP) ensures the function of critical metabolic enzymes, PDH, α-KGDH, and TKT. Reduced cellular TDP promotes neurodegeneration characterized by severe deficits in cerebral energy metabolism, inflammation, oxidative stress, and an increase in plaque formation within the hippocampus, cortex and thalamus (1-30,68,69). The activity of TKT, PDH, α-KGDH are also significantly reduced in post-mortem Alzheimer's patients and strongly correlate with dementia rating (20,31,32). Downregulation of myelination-related genes in the frontal cortex was also detected in thiamine deficient rats consistent with that observed in postmortem AD patients (70,71). Several clinical case-control studies have also demonstrated reduced T/TDP levels in AD patients (9,12,72). These clinical correlations are strongly linked by compelling preclinical data linking TI induced AD-neuropathological hallmarks such as increased BACE1 activity, increased Aβ deposition, and Tau hyperphosphorylation (1-5,73).

Why thiamine levels are reduced and how TI induces AD pathology is unclear and multifactorial. Reduced intestinal absorption and increased thiamine phosphatase activity may be a contributor to declining plasma levels of thiamine during aging and AD (74-76). However, nutritional status and presence of age related co-morbidities do not significantly correlate with reduced thiamine levels in elderly patients (13). Changes in thiamine transport and kinase expression and activity, such as SLC19A3 and TPK1 may also contribute to reduced cellular TDP and inducing neuropathology (77,78). Supplementation with the thiamine mimetic Benfotiamine has also shown significant promise in preclinical and clinical AD studies for improving cognitive function (79-83). Benfotiamine supplementation increases thiamine/TDP levels, improve metabolic markers such as glycation end products, and reduce oxidative stress through a possible non-cofactor mechanism (79,80,84-87). Supported in part through our previous grant (R21AA021948), we have uncovered TI induced HIF1α as a potential mechanism for TI induced AD neuropathology (34-36).

Under normal oxygen tension, hydroxylation by HIF-prolyl hydroxylases (HIF-PHDs) and subsequent binding of the Von Hippel-lindau tumor suppressor promotes ubiquination and proteasomal degradation of HIF1α (38,39) (Fig.1). When cells experience reduced oxygen tensions, HIF1α protein is stabilized and forms a heterodimer with HIF1β. The resulting HIF1 complex regulates expression of numerous genes including those involved in cell survival and cell death (38,39). ***However, stabilization of HIF1α and induction of HIF1 regulated gene expression is also metabolically controlled in part by the accumulation of the intermediate pyruvate, even in the presence of normal oxygen*** (88,89). Reduced activity of PDH and pyruvate accumulation has been well characterized during TI (90-95). Our published findings demonstrate that pyruvate accumulation is directly responsible for TI induced HIF1α activity and expression of target genes (36). Pyruvate buildup inhibits HIF-PHDs activity by competing with the required cofactor α-ketoglutarate (96-98) (Fig.1). To further establish the role of HIF-PHD inhibition during TI, the addition of the cell permeable octyl-α-ketoglutarate (KG) significantly attenuated TI mediated HIF1α stabilization and expression of established amyloidogenic, pro-inflammatory, and pro-apoptotic target genes, such as MCP1, BNIP3, and BACE1 (Fig.2A) (97-99). No significant increase of two additional stress response factors regulated by HIF-PHDs, ATF4 or NFkβ within HT22 cells was observed (Fig.2A) (100-103). Similarly, shHIF1α knockdown also limited activation of HIF1α and expression of BNIP3 and BACE1 (Fig.2B). Stability of HIF1α-OH form was reduced with HIF-PHD inhibitor DMOG and with TI treatment that was restored when combined with KG (Fig.2C). Coupled with our published work in primary astrocytes and neuronal cell models, this further indicates the ability of TI to induce HIF1α regulated pro-apoptotic and amyloidogenic genes (34-36).

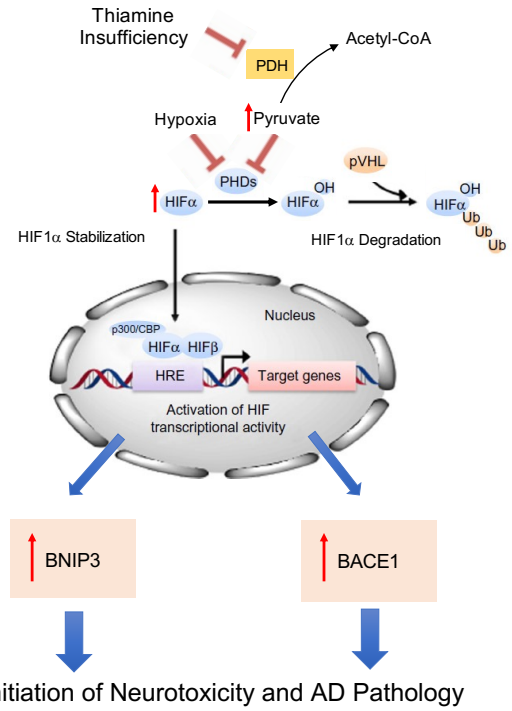

Figure 1: Metabolic activation of HIF1α. Inhibition of pyruvate dehydrogenase (PDH) due to thiamine insufficiency increases intracellular pyruvate that can block hydroxylation of HIF1α by prolyl hydroxylase (PHD) preventing degradation. Chronic stabilization and activation of HIF1α in turn can mediate pro-apoptotic and amyloidogenic gene transcription.

HIF1α is an essential adaptive stress response transcriptional factor that can contextual mediate either pro-survival or pro-death cellular responses. Acute/early HIF1α driven responses within ischemic stroke models can

limit neurological injury (104-106). In contrast, pre-existing hypoxic stress events and prolonged HIF1α activation are associated with promoting apoptosis, neurological injury, and increased prevalence for the development of AD pathology (45-50,107-111). ***The chronic nature of reduced thiamine levels in pre-dementia patients may produce chronic HIF1α activation that promotes AD-neuropathology.*** In contrast, activation of HIF1α through HIF-PHD inhibition has been suggested to limit cellular toxicity induced by Aβ (112-115). However, this neuroprotective benefit from pharmacological inhibition of HIF-PHDs can function independently of HIF1α transcriptional activity (115-117). Reduced ferroptosis and/or iron participation in plaque pathology using HIF-PHD iron chelator inhibitors may be driving this neuroprotective benefit (118-120). ***This dichotomy in HIF1α underscores the critical need for further research that can codify a contextual perspective that drives either HIF1α neuropathology or protection during TI. Unfortunately, there is a significant gap in our knowledge for the circumstantial relationship between TI stress and HIF1α activation.*** The premise to study TI associated neurotoxicity and AD pathology is significant given the expected rise in AD cases due to an aging population and the strong association of thiamine levels with AD outcomes. Overall, this contribution is the first step in a continuum of research that is expected to further our knowledge towards a mechanistic understanding of TI neuropathologies.

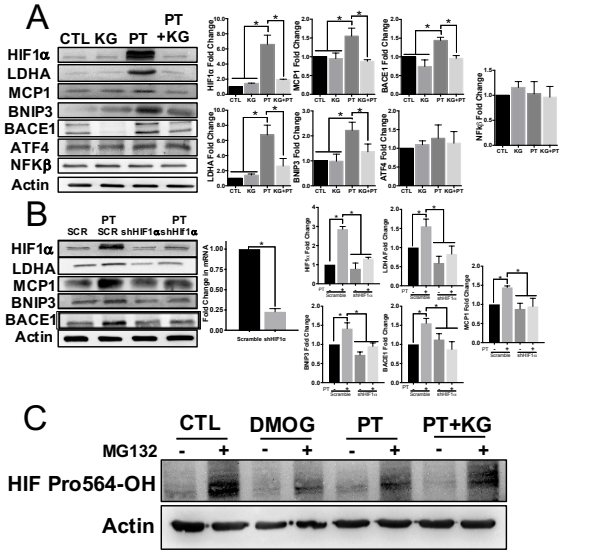

Figure 2: (A) Representative Western blot and densitometry from N=3 independent replicates from mouse hippocampal cells (HT22) treated with either 3μM thiamine containing RPMI1640 media (CTL), 2mM Octyl-α-ketoglutarate (KG), 10μM PT, or PT+KG for 3 days. (B) Representative Western blot and densitometry from N=3 independent replicates from shHIF1α-HT22 and SCR-HT22 control cells treated with either 3μM thiamine containing RPMI1640 media (CTL) or 10μM PT for 3 days. Fold change in HIF1α mRNA in shHIF1α HT22 compared to SCR was assessed using qRTPCR. (C) HIF1α-OH stabilization with 10μM MG132 (4h) in HT22 cells treated for 3 days with 150μM DMOG, 10μM PT, or PT+2mM KG. (★) Represents a statistically significant difference of $p<0.05$ based on the results of a one-way ANOVA with Tukey's post-hoc test.

INNOVATION

Previous work on TI has provided only a descriptive evaluation for neurological injury. Our innovative approach and hypothesis dives deeper into the investigation of a mechanistic initiator and goes beyond the simple descriptive assessment of TI neurotoxicity. Addressing this shortcoming is an important issue from a nutritional, pathological, and therapeutic perspective. The recognition of reduced thiamine plasma levels clinically with aging and correlation with AD diagnosis and cognitive impairment, heightens the impact and importance to understand the factors driving the initiation of neurological injury and AD pathology as a result of TI. Investigating the contextual relationship between TI and HIF1α represents a substantive departure from current paradigms for HIF1α in AD research. Conceptual and technical innovations in the field of thiamine biology and related neurodegeneration include: (1) The influence of TI and HIF1α as a novel unifying mechanism for both the metabolic and amyloidopathy associated with AD. (2) Utilization of neuronal and glial Cre-drivers to understand the cell-to-cell relationship of HIF1α activation during TI to mediate neurotoxicity. (3) Establishing the graded level of TI to mediate cell specific HIF1α responses and onset of neuropathology. State-of-the-art methodology including RiboTag RNA-Seq and MR Imaging coupled with cell specific Cre-drivers for HIF1α knockout and triple transgenic AD mouse model are highly innovative in the field of thiamine biology.

APPROACH

Dietary Restriction Model: Although reduced nutritional intake is one factor contributing to reduced thiamine status, prolonged intake of diets devoid of this micronutrient would be an extreme case and not completely representative of the clinical situation. Blood levels of TDP demonstrated a significant positive correlation with MMSE score in elderly patients (12). Therefore, uncovering the molecular phenotype relating the degree of TI would be of considerable significance. ***The degree of TI capable of inducing neuropathology is highly desired in the field.*** Utilization of TI model systems providing complete depletion of thiamine or using the structural analog and anti-thiamine compound, Pyrithiamine (PT), are effective to establish TI AD-neuropathology (1,4,5). PT treatment is severe and aggressive *in vivo*, with significant neuropathy and death occurring within 10-12 days that can limit the detectability for the temporal onset and ability to titrate and correlate with thiamine status (TDP levels and TKT activity). To address this shortcoming, **throughout this application (Aims 1, 2, and 3)** we will use a graded dietary restriction approach to achieve varying degrees of thiamine status in our mouse models. This will provide more clinically relevant insight into the degree of thiamine status on HIF1α induced AD-neuropathology. We will base our dietary intake levels on the nutrient requirement of

thiamine being 10μg/day for mice (121). Mice will receive a diet supplemented to provide 0 (TI), 0.001 (moderate TI), 0.01 (mild TI), compared with 10μg/day of thiamine (CTL). These graded thiamine levels will be supplemented into a custom formulated thiamine deficient liquid chow diet based on product #F1268SP AIN-76 (Bio-Serv). Liquid diet was chosen as it provides a more suitable way to control the amount of thiamine consumed by avoiding potential aversion to water dosing and minimizing pain/distress from long term daily injections or gavage. Animals will be monitored daily, and the volume of food consumed per mouse calculated. The volume of food provided, and amount of thiamine supplemented will be based on the cohort with the lowest amount of food consumed to ensure isocaloric intake across all groups. Previous studies have demonstrated that limited mastication and liquid diets can alter glucose metabolism (122,123). To control for the impact of diet change to liquid, we will include a group of mice maintained on solid chow diet (10 μg/day of thiamine). If we observe significant differences in glycolytic gene expression between our control solid and liquid diets, we will modify our approach to obtain custom formulated solid diet containing varying thiamine compositions. Figure 3 demonstrates that 4 weeks of 0T was capable of inducing HIF1α in C57BL/6 mice.

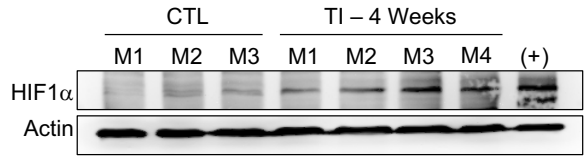

Figure 3: Thiamine restriction (TI) for 4 weeks induces HIF1α in thalamus of female C57BL/6 mice. Western blot of thalamic tissue from 11 mth old C57BL/6 mice pair fed either normal diet (CTL, N=3) or thiamine deficient (TI, N=4) diet for 4 weeks. Actin was used as loading control and positive control for HIF1α (+) was DMOG treated HT22 cells.

Aim 1: Neurological injury mediated by chronic thiamine insufficiency involves cell autonomous and non-autonomous effects of HIF1α between astrocytes and neurons

Introduction: HIF1α activation is a critical stress response that can provide neuroprotective or pathological gene expression under various situations. Early-stage gene expression during hypoxia or sublethal Aβ involves initial adaptive responses and late stage or high dose Aβ promotes pro-apoptotic gene expression, such as BNIP3 (104,112-115,124-130). Cell specific responses have also been described for HIF1α (131). Induction of HIF1α in astrocytes can promote neuronal toxicity and loss of HIF1α function in astrocytes protected neurons from hypoxic damage (132). Temporal onset of HIF1α during hypoxia was described early in neurons but slow and long lasting in astrocytes (133). This is congruent with the early phase loss of neurons that precedes reactive astrogliosis and ultimately astrocyte loss during late-stage TI (134,135). Inhibition of PDH activity by TI within astrocytes could enhance lactate production via HIF1α regulated LDHA which can mediate neuronal toxicity and the formation of histological lesions (136). The lactate transporter MCT4 found in astrocytes is also a HIF1α regulated gene that could enhance extracellular deposition of lactate and contribute to neuronal injury (137,138). This "lactate storm" is also associated with contributing to neuronal toxicity in TBI and could explain why glucose administration to TI patients can exacerbate neurological injury (139,140). **Unfortunately, no study has investigated the relationship of astrocytes and neurons during TI because no testable mediator has been recognized until now.** Therefore, *the objective of this aim* is to determine the involvement of HIF1α activation to facilitate neurotoxicity during TI stress. Our *working hypothesis* is that HIF1α activation within astrocytes during chronic TI enhances neuronal death. Previous studies have established knockout or inhibition of HIF1α can attenuate neurotoxicity, therefore our *approach* will be to cell selectively knockout HIF1α within either astrocytes or neurons to ascertain the temporal onset, thiamine status, and cell type relationships driving TI induced neurotoxicity

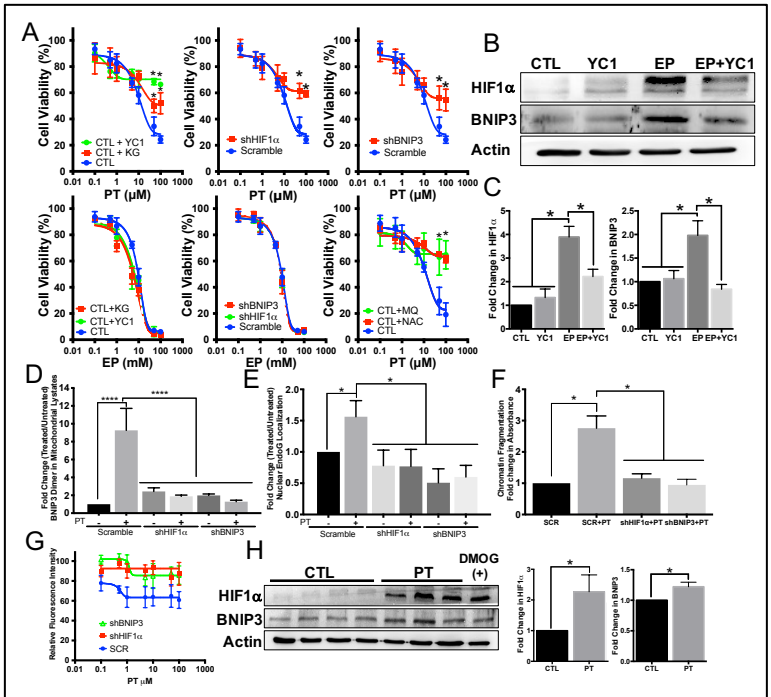

Figure 4: (A) Cell viability measured by MTT assay on shHIF1α, shBNIP3, and scramble control HT22 cells treated with PT, +10μM YC1, +2mM octyl-α-ketoglutarate (KG), +1uM MitoQ, or 100uM NAC for 3 days. (B) Representative WB and (C) densitometry from N=3 independent replicates of HT22 treated with either CTL, 10μM YC1, 1mM EP, or EP+YC1 for 3 days. (D) Densitometry from N=3 independent replicate WB's from shHIF1α, shBNIP3, and scramble control HT22 for BNIP3 dimer (60kDa) in mitochondrial lysates and (E) EndoG in nuclear lystates treated with either CTL or 10μM PT for 3 days. (F) DNA fragmentation ELISA kit (Roche Applied Sciences) according to the mfgs protocol. shHIF1α, shBNIP3, and scramble control HT22 cells were treated with 10μM PT for 3 day. (G) potentiometric dye tetramethylrhodamine methyl ester (TMRM) was used to assess changes in mitochondrial membrane potential (MMP). After 72h of PT treatment to shHIF1α, shBNIP3, and scramble control HT22 cells, 50 nM of TMRM was added for 30min, rinsed, then cellular fluorescence was measured at Ex/Em=550/575 nm. (H) Representative WB and densitometry of whole brain from 11-mth old C57BL/6 mice injected IP daily for 7 days with 10mg/kg PT or vehicle (CTL). Whole brain from mice treated with 200mg/kg DMOG for 3 days was used as positive control. Each lane presents one mouse. (★) Represents a statistically significant difference of $p<0.05$ based on the results of a one-way ANOVA with Tukey's post-hoc test for and T-test for (H).

(106,129,141-144). *We expect* to establish the functional involvement of HIF1α as an underlying initiator for TI neurotoxicity and delineate the impact of astrocytic and neuronal HIF1α activation.

Justification, Feasibility, and Preliminary Data: Intriguingly, there is an overwhelming degree of congruency in the cellular responses leading to neurological damage between ischemia and TI. Both hypoxia and TI lead to excitotoxicity via decreased GLT1 and GLAST activity in astrocytes (145-150). HIF1α induces expression of AQP4 and MMP9 during cerebral ischemia leading to brain swelling and TI also produces focal edema that correlates with increased AQP4 and MMP9 expression (151-155). Neuroinflammation is also a component of hypoxia, AD, and TI resulting in chemokine and pro-inflammatory cytokine expression (17,156-159). Astrocytes can produce various pro-inflammatory cytokines including TNFα, IL6, and IL1β in response to TI, hypoxia, and other stresses (134,160-162). Inhibition of HIF-PHDs activity can promote NFkβ activity and induce pro-inflammatory cytokine expression (100,101). TI induced pyruvate and subsequent HIF-PHDs inactivation could account for TI induced inflammation. Additionally, expression of the pro-inflammatory chemokine, monocyte chemoattractant protein-1 (MCP1) has also been demonstrated in response to TI and hypoxia (163,164). HIF1α is a direct transcriptional regulator of MCP1 expression (42,165).

Using isolated primary mouse astrocytes, we have published that HIF1α activation and induction of the pro-apoptotic proteins BNIP3, NIX, NOXA, and the pro-inflammatory chemokine MCP1 during TI (35). Cell proliferation of HT22 cells was reduced by PT treatment but improved in the presence of the HIF1α inhibitor YC1, HIF-PHD activator KG, shHIF1α, and shBNIP3 KD (Fig.4A). Interestingly, the cell permeable ethyl-pyruvate (EP) increased HIF1α and BNIP3 expression that was attenuated by YC1 but EP toxicity to HT22 cells could not be attenuated by shHIF1α, shBNIP3, YC1, or KG (Fig.4B+C) (166). This finding is consistent with HIF1α/BNIP3 requiring oxidative stress to mediate cell death (110,167). This was confirmed with the attenuation of PT toxicity using antioxidants MitoQ and N-acetyl-Cysteine (NAC) (Fig.4A). TI is well established to induce oxidative stress suggesting that HIF1α/BNIP3 pathway may be a central component for TI neurotoxicity (26,35,135,168). Consistent with BNIP3 mediated apoptosis, PT stimulated BNIP3 dimerization and translocation to the mitochondria (Fig.4D), EndoG release (Fig.4E), and DNA fragmentation (Fig.4F), and increased mitochondrial membrane polarization (Fig.4G) that were all decreased with shHIF1α and shBNIP3 KD in HT22 cells. Stabilization of HIF1α and BNIP3 protein was increased in whole brain samples of TI treated mice (Fig.4H). Unfortunately, the *in vivo* relationship between astrocytic and neuronal HIF1α during TI is unknown.

Research Design: To determine the contribution of HIF1α mediated pro-apoptotic responses in TI associated neurotoxicity within astrocytes and neurons we will employ a tamoxifen inducible system to conditionally knockout HIF1α. This will avoid loss of function effects on embryonic neuronal developmental, allowing for selective loss after the mice reach full CNS development and adulthood. Cell selective knockout of HIF1α will be achieved by crossing HIF1α$^{f+/f+}$ (Jackson Labs - B6.129-HIF1α^{tm3Rsjo}/J) mice with the tamoxifen inducible GFAP-CreERT2 (Jackson Labs B6.Cg-Tg(GFAP-cre/ERT2)505Fmv/J) and Syn1-CreERT2 (Riken-B6.CgTg(Syn1creERT2)1Tfur) to remove HIF1α from mature astrocytes and neurons, respectively. Age related differences in the responses to TI have been reported, with the greatest response occurring in older mice than in young mice (169-171). Moreover, AD and other dementias occur greater in elderly women than males, suggesting sex differences in the onset of neuropathology (172). Therefore, homozygous HIF1α floxed male and female mice at 15 mos. of age (~50 human yrs.) will be used and will be analyzed collectively and separately (173). Homozygous HIF1α floxed mice will be randomly divided into either an experimental arm or control arm. Mice in the *experimental arm will be dosed with tamoxifen IP* at 75mg/kg/day in corn oil for 5 days to facilitate loss of HIF1α. The *control arm will be dosed IP with vehicle* (corn oil) at a volume consistent to the tamoxifen dose given in the experimental arm. Following a conditioning period to normal control liquid diet (2 weeks), mice will be randomly divided into each dietary restriction group. Mice will be fed these diets for up to 12 weeks with mice subjected to assessments described below every 7-14 days depending on the thiamine diet level. The length of time was chosen to provide a sufficient interval for responses in the mild/moderate TI groups, which can take longer than the expected 4/5-week onset with TI (0 T) (174-177). Assessments every 7 days with the TI (0 T) group and 14 days for the moderate/mild and CTL group will provide a temporal relationship for the onset of HIF1α activation and transactivation of target genes based on thiamine intake levels. This will minimize the number of total animals used. However, we will use an iterative approach that will adjust the feeding time frame and assessment interval based on outcomes. With an anticipated 2-fold change, sigma of 0.4, and power of 0.8, we calculate using a minimum of n=4 male and n=4 female mice per diet group/time point.

Preconditioning with the HIF-PHD inhibitor DMOG: HIF-PHD2 knockout and preconditioning with HIF-PHD inhibitors can limit neurological injury due to protective gene expression prior to the stress condition (178-181). Since acute HIF1α activation can induce survival responses, we will perform preconditioning studies with the HIF-PHD inhibitor Dimethyloxalylglycine (DMOG) to differentiate between survival or apopototic HIF1α

responses induced during TI. DMOG pretreatment has been shown to reduce infarct size and limit neurotoxicity prior to ischemia or glutamate induced apoptosis (182-185). Control and floxed mice will be treated with 200mg/kg DMOG IP for 3 days (or vehicle control) prior to initiation of TI diet to determine if acute HIF1α can delay the onset of TI neurotoxicity. Our preliminary results demonstrate an increase in HIF1α in whole brain samples after 3 days of 200mg/kg DMOG (Fig.2G).

1.1. Physical assessment of neurological injury: Common signs and symptoms of neurological injury during TI in animal models include ataxia, loss of righting reflex (LORR), anorexia, and weight loss (186-189). Mice will be evaluated every day for body weight and food intake following diet change into our dietary restriction group and pair fed controls as stated above. The intent of this evaluation will be to quantify the onset and severity of the physical symptoms of neurological damage due to TI and the presence or absence of functional HIF1α within astrocytes or neurons. Assessments for both ataxia and LORR will be done using a blinded observer approach. We will use a reported grading scale method to determine the extent of ataxia based on a ledge test (190). LORR will be defined as mice taking greater than 30sec to right itself after placement on its back in a V-shaped trough (191,192). Pre-symptomatic encephalopathy is typically defined upon the onset of ataxia which progresses to the symptomatic phase characterized by a LORR and possible onset of seizures (136,193). Mice that have a graded ataxia score >2 and an LORR > 30sec will be considered to be symptomatic.

1.2. Measurement of Thiamine Status: We will utilize HPLC with pre-column derivatization and fluorescence detection to profile thiamine (T), thiamine monophosphate (TMP), and thiamine diphosphate (TDP) levels using a previously published method by our group in collaboration with our co-investigator Dr. Michael Bartlett (194). Our goal is to quantify T/TMP/TDP to establish that our dietary restriction model produces a progressive reduction at each time point in whole blood (obtained at time of euthanization) as it is highly correlated to established enzymatic functional tests for thiamine status (195). Levels of T/TMP/TDP will also be measured in whole brain and isolated brain regions including but not limited to cortex, thalamus, and hippocampus. Evidence indicates that TI diet restriction can reduce T/TDP blood levels (174). We will also quantify the activity of thiamine dependent enzymes, PDH, αKGDH, and TKT in isolated brain regions and TKT in whole blood using our previously established methods (36,87).

1.3. Measurement of Pyruvate and Lactate: Our published *in vitro* results have established that TI can increase pyruvate and extracellular lactate levels (34). Quantitation of pyruvate will be performed utilizing a pyruvate assay as previously published by our lab (34,36). Changes in pyruvate will be associated with the regional and temporal induction of HIF1α activity. An increase in LDHA in neurons and astrocytes and lactate accumulation has been observed in TI animal models demonstrating that de novo synthesis of lactate occurs in the brain and not the periphery (136). This “lactate storm” is also associated with contributing to neuronal toxicity and could explain why glucose administration to TI patients can exacerbate neurological injury (139,140). Since LDHA is a direct HIF1α regulated gene, knockout of HIF1α in either astrocytes or neurons may provide evidence of cell type specificity for TI induced lactate production. Knockout of HIF1α in either astrocyte or neurons and controls will be infused with glucose (500mg/kg IP) to promote lactate production (136). This will be done on the day of assessments. Quantitation of lactate 60 min post infusion in whole brain, isolated brain regions (thalamus, cortex, hippocampus), and whole blood (periphery control) will be done using lactate assay previously published by our lab (34). LDH expression changes due to TI and HIF1α knockout will be established using qRTPCR and WB. To distinguish changes in LDH expression due to TI and HIF1α knockout we will utilize IF dual labeling with either GFAP or NeuN as a marker for astrocytes and neurons (Aim 1.7 for further analytical details.

1.4. MRI imaging of neurological injury: To characterize the progression of TI related neurotoxicity and the impact of HIF1α knockout in either astrocytes or neurons, we will perform longitudinal magnetic resonance imaging (MRI) measurements. Our co-investigator Dr. Qun Zhao at the UGA Bio-imaging Research Center will be responsible for all MRI experiments. Repetitive measurements will be performed on the same mouse to serve as their own controls and comparators for the temporal progression of neurological injury. MR scanning will be performed on mice every 7 days for 60-90min using a Varian 7T/21 cm inner diameter horizontal bore magnet equipped with a Direct Drive console. To assess the progression of neurological damage and detect the earliest changes, different quantitative MR imaging will be performed, including: (1) Quantitative brain T_2/T_2* mapping to study potential time-dependent lesions and microstructural properties of multiple regions of interest (ROI) such as thalamus, lateral ventricles, and inferior colliculi. (2) Quantitative brain T_2-FLAIR to characterize TI induced edema. (3) To assess tissue damage, diffusion tensor imaging (DTI) will be conducted to study molecular displacement, extracellular space and intracellular volumes and apparent diffusion coefficient (ADC) and fraction anisotropy (FA) maps will be estimated. We anticipate that a temporal change in FA and ADC maps may reflect variations in microstructure and degeneration of axons. In addition, it has been reported that connectivity

properties change in an ordered manner over the course of the disease, and AD patients showed altered small-world architecture in the structural cortical network (196,197). We therefore plan to investigate brain's structural connectivity, particularly the small-world architecture and topological organization of the control and floxed mice using our recently proposed machine learning models and graph theory (198). In a proof of concept preliminary study, C57BL/6 mice were pair fed with TI diet and injected daily IP with PT or thiamine (CTL) for up to 10 days (Fig.5). Mice were evaluated using MRI by our co-investigator (Dr. Qun Zhao) on day 10. A significant increase ataxia score and the T_2-weighted hyper-intensity was observed in the thalamus with PT compared to control (Fig.5A+B). These findings are consistent with previous reports demonstrating TI induced neurological damage using MRI (188,199). Western blot of thalamic tissue demonstrated an increase in HIF1α expression with PT treatment (Fig.5C). This preliminary study demonstrates our feasibility to measure neurological injury using MRI.

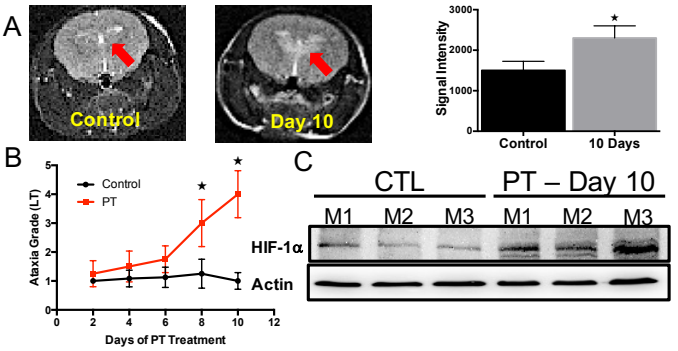

Figure 5: Neurological injury and HIF1α induction in pyrithiamine treated mice. C57BL/6 were pair fed with TI Lieber-DeCarli liquid diet and injected daily IP with either 0.5mg/Kg pyrithiamine or thiamine (CTL) for 10 days. (A) T2-weighted MRI Images (control and TD day 10) indicating increased thalamic signal hyper-intensity (Red arrow) and quantitative thalamic MR signal hyper-intensity from N=3 mice. (B) Blinded observer measurement of ataxia using ledge test. (C) Western blot of HIF1α from N=3 mice with actin as loading control. (★) Statistical significant differences with $p<0.05$ using unpaired T-test.

1.5. Assessment of cellular/tissue damage: Multiple histological assessments will be performed to determine the effect of cell selective HIF1α knockout on neurotoxicity during TI. Briefly, mice will be transcardially perfused with 4% PFA. Excised brain placed in 25% sucrose with 4% PFA solution flash frozen and stored at -80^{0}C. Mouse brains will be coronal sliced ranging between Bregma level -2.0 to -1.0 using a cryostat. Slice thickness, fixation, permeabilization, blocking, and other processing parameters will vary depending on the assay and manufacture protocols. Assessments of neurotoxicity include H&E and Fluoro-Jade C staining. Apoptosis will be assessed using an *in situ* TUNEL assay to measure apoptotic nuclei. To further verify apoptotic cells, Hoechst 33258 staining will be employed to identify apoptosis on the basis of changes in nuclear morphology, such as chromatin condensation and fragmentation. For cell specific evaluations we will probe for NeuN immunoreactivity and cresyl violet staining of Nissl substance for neurons. A reduction in signal from either would indicate neuronal damage/loss. Reactive astrocytes will be assessed by immunoreactivity for GFAP. The loss of surrounding neurons may lead to astrogliosis (200). Alternatively, astrocyte death as a consequence of TI may result in a GFAP decrease (134). For quantification of IHC/IF, marker intensity of at least three random fields from 5 serial sections for each brain will be determined.

1.6. Behavioral assessment: The contribution of HIF1α during TI on cognitive/memory deficits will be assessed using the Barnes Maze (BM) for spatial memory and learning and Novel Object Recognition (NOR) for short term recognition memory. These cognitive assessments are to be performed using methods previously published by our co-investigator, Dr. Nikolay Filipov (201,202). Since pathological brain changes at early time frames are not expected to produce significant effects on learning and memory tasks, mice will begin assessment after 28 days of treatment to provide a fixed time frame for neurological injury. *Once animals reach the indicated time frame of treatment, they will receive a single 50mg/kg IP injection of thiamine and switched back to full control thiamine diet. The rational of returning thiamine restricted mice back to normal thiamine levels is to avoid further progression in neurological damage that can progressively impact the training phase or result in death.* Briefly, for BM mice were habituated to the maze one day prior to the acquisition phase. During the acquisition phase, mice were trained to learn and escape via a target hole (TH). For the probe trial, the TH was removed, and mice freely explore the maze. The average and total errors made, time to reach TH, and distance to TH will be analyzed. For NOR training phase, mice are placed in the open field arenas in the presence of two identical objects and were allowed to explore them for 5 min. After 1h rest in their home cages, mice are placed back into the arenas with one familiar and one novel object and allowed to explore them for 5 min. Number of approaches with the familiar or novel object, and time spent exploring the familiar or novel object will be determined.

1.7. Expression of HIF1α regulated target genes: Stabilization of HIF1α leads to target gene expression involving both prosurvival and proapoptotic responses. We will establish in the presence and absence of functional HIF1α the expression of known HIF1α regulated genes via WB, IF, and qRT-PCR. Adaptive HIF1α target genes involved in angiogenesis (VEGF), glycolysis (ENO1), glucose transport (GLUT1,3), and erythropoiesis (EPO) will be measured (39). Expression of HIF1α regulated thiamine homeostasis genes SLC19A3 and TPK1 will also be quantified (87,203). Pro-apoptotic/necrotic protein expression during TI will

quantify changes in BNIP3, NIX and NOXA using WB, IF, and qRT-PCR. We will also determine BNIP3 in mitochondrial lysates to determine the functional activation of BNIP3 during graded TI using established methods (Fig.4D). Apoptotic markers such as caspase 3/7 activity will also be measured using a Caspase-Glo 3/7 kit as done previously (35). Cell dependent expression of BNIP3, NIX, or NOXA expression will be determined using IF and dual labeling with either GFAP or NeuN as a marker for astrocytes and neurons. Briefly, mice will be transcardially perfused with 4% PFA. Excised brain will be placed in 25% sucrose with 4% PFA solution, flash frozen, and stored at -80^{o}C. Mouse brains will be coronal sliced ranging between Bregma level -2.0 to -1.0 using a cryostat and processed for IF staining. Marker fluorescence will be analyzed with a Nikon Microscope Eclipse Ti. For quantification, the fluorescence intensity of at least three random fields from 5 serial sections for each brain will be determined using ImageJ software. Neuroinflammation and MCP1 expression is also a component of hypoxic/ischemic stroke and HIF1α has been established to be a direct regulator of MCP1 expression (42,165). Induction of MCP1 during TI activates microglia to secrete IL1β and TNFα that is implicated in mediating neuronal death (17). To establish if TI mediated HIF1α activity in astrocytes and/or neurons facilitates proinflammatory responses, we will quantitate changes in MCP1, IL1β and TNFα by qRTPCR.

1.8. Oxidative stress measurement: A critical factor required for HIF1α mediated apoptosis via BNIP3 is the presence of oxidative stress (Fig.4) (110,167). TI is well established to induce oxidative stress as a component for neurotoxicity (26,35,135,168). Therefore, we will quantify the extent of oxidative stress during TI and HIF1α knockout. Oxidative stress will be measured by detecting lipid peroxidation (TBARS) and nitrate modifications of proteins (nitrotyrosine levels) using established methodology (204,205). The regional and cellular HIF1α/BNIP3 expression will be correlated with the extent of oxidative stress.

Anticipated results, potential pitfalls, and alternative approaches: The objective of this aim is to establish the involvement of HIF1α activation to mediate neurotoxicity during TI. By employing cell type selectivity of HIF1α KO we expect to delineate the cell-to-cell relationships between astrocytic and neuronal HIF1α activation during TI. We expect that feeding TI diet will produce significant increase in pyruvate (aim 1.3), progressive reductions in T/TDP levels, and reduced activity of TDP dependent enzymes (aim 1.2). Collectively we expect that knockout of either astrocyte or neuronal HIF1α will attenuate and delay the onset of neurotoxicity compared to WT (aim 1.1, 1.4, 1.5, 1.6). These outcomes will confirm our hypothesis for HIF1α to initiate neurotoxicity during TI. However, the temporal and magnitude relationship of neurotoxicity is expected to be early and greater with neuronal knockout compared to astrocytic knockout. This outcome is expected due to loss of astrocytic HIF1α producing neuroprotective results (132). We also expect that the expression of HIF1α regulated pro-survival, pro-apoptotic, neuroinflammatory genes and production of lactate will be reduced within HIF1α null astrocytes and neurons during TI as demonstrated previously (106) (aim 1.3 and 1.7). We also expect that preconditioning the induction of HIF1α prior to TI will delay the onset of neurotoxicity due to the early onset of adaptive survival genes in particular with low grade TI. However, chronic high degree of TI and subsequent oxidative stress is expected to mediate HIF1α/BNIP3 mediated neurotoxicity. Lastly, we expect the extent of oxidative stress to correlate with the degree of TI and to accompany HIF1α/BNIP3 expression and mitochondrial localization in regions exhibiting cell death (aim 1.8).

Although our preliminary *in vitro* data strongly supports the induction of HIF1α during TI as an underlying regulator for neurological injury, there is a remote possibility that it could be invalidated when objectively tested *in vivo*. Neuronal expression of HIF2α can function as a redundant pro-survival pathway during HIF1α KO in neurons (106,206). HIF2α has been associated with pro-apoptotic signaling in tumor tissue and dual knockout of HIF2α and HIF1α improved neuronal cell survival in an ischemic mouse model (106,206). Our preliminary and published *in vitro* findings have demonstrated that TI does not appear to involve induction or nuclear translocation of HIF2α (35). We would evaluate the role of HIF2α during TI *in vivo* using a similar approach by cell selective knockout of HIF2α (Epas1^{tm1Mcs} – Jackson labs).

Aim 2: Limiting HIF1α activation delays the onset of thiamine insufficiency associated AD-like neuropathology.

Introduction: Although primarily involving the cortex and hippocampus, thalamic amyloid deposits and NFT pathology has also been observed in AD brains (28-30,207). An increase in Aβ plaque deposition occurs during TI within the thalamus, hippocampus, and cortex (1-5,73). An increase in BACE1 expression was also observed in whole brain extracts of plaque competent Tg19959 transgenic mice as a consequence of TI (1). HIF1α directly trans-activates the expression of BACE1 leading to plaque formation and initiation of amyloidogenic processes (43,46,208). Tau hyperphosphorylation is another characteristic pathological alteration occurring in AD (209). Both hypoxia and TI increase Tau phosphorylation as a pathological contributor in AD progression (2,47,107). The *objective for this aim* is to determine if HIF1α activation during TI is an initiator for AD neuropathology. Our *working hypothesis* is that pharmacological inhibition of HIF1α limits plaque deposition and delays the onset of

AD neuropathology during TI. Our approach will be to administer YC1 as a prototypical HIF1α inhibitor and determine the impact on TI induced AD pathology using the 3xTg-AD mouse model. *We expect* that inhibition of HIF1α activity during TI can delay the onset and/or reduce the extent of plaque deposition and formation of NFT pathology. **Such a finding would establish HIF1α as a critical pathogenic initiator for TI induced AD neuropathology and provide evidence for a potential synergistic therapeutic intervention with thiamine mimetics**.

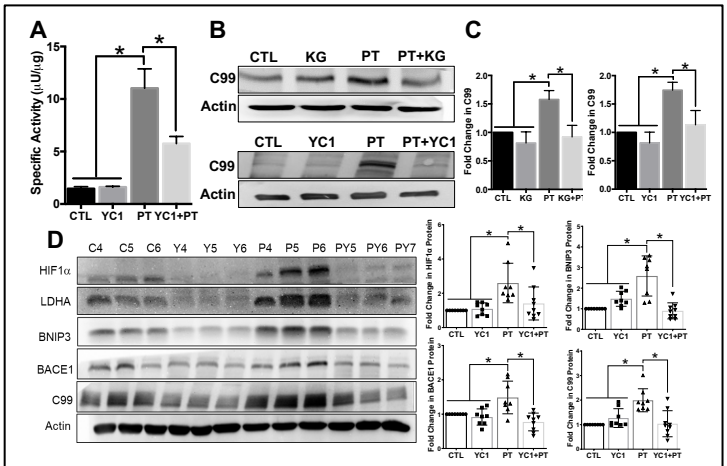

Figure 6: (A) Bace1 activity in Mouse hippocampal HT22 cells treated with either 3μM thiamine containing media (CTL), 10μM YC1, 10μM PT, or both YC1 and PT for 3 days. (B) Representative Western blots of APP cleavage fragment C99 in HT22 cells treated with either CTL media (CTL), 10μM YC1, 2mM octyl-a-Ketoglutarate (KG), 10μM PT, YC1+PT, or KG+PT for 3 days. (C) Densitometry from N=3 independent expts. (D) Representative WB from whole brain for HIF1α, LDHA, BNIP3, BACE1 and C99 samples from 3 month old 3xTgAD mice injected either saline (C4-6), 5mg/Kg YC1 (Y4-6), 2mg/kg PT (P(4-6), or both PT and YC1 (PY4-6) for 10 days. Included is densitometry from N=9 mice per group normalized to actin control. (★) Represents a statistically significant difference of $p<0.05$ based on the results of a one-way ANOVA with Tukey's post-hoc test.

Justification, Feasibility, and Preliminary Data: Evidence has established that TI promotes AD-neuropathology associated with increased BACE1 activity, increased Aβ deposition, and Tau hyperphosphorylation (1-5,73). Our preliminary results in mouse hippocampal neuronal HT22 cells establish an increase in BACE1 protein and mRNA expression that can be attenuated with either HIF-PHD activator KG, HIF1α inhibitor YC1, and shHIF1α (Fig.2A/B+7A). The increase in expression resulted in an increase in BACE1 activity that was attenuated by YC1 (Fig.6A). Consequently, an increase in BACE mediated APP cleavage product C99 (β-CTF) was observed in HT22 cells that was significantly reduced with KG and YC1 (Fig.6B+C). To determine if TI activates HIF1α *in vivo*, 3xTgAD mice were administered PT +/- YC1 IP daily for 10 days (Fig.6D). PT treatment activated HIF1α and induced LDHA, BNIP3, BACE1 and C99. Co-administration of YC1 with PT significantly attenuated HIF1α activation, expression of LDHA, BNIP3, BACE1, and production of C99. Since PT is an aggressive approach to induce TI our experimental design will be adjusted to accommodate our chronic graded dietary deficiency model (earlier age of mice, lower dose of YC1). Overall, this demonstrates the feasibility and role of HIF1α in TI to induce genes/proteins associated with AD neuropathology.

Research Design: The 3xTgAD strain that will be used in this study is the first transgenic animal model to develop both plaque and NFT pathology in AD-relevant brain regions in an age-dependent fashion, which closely resembles AD initiation and progression in humans (210,211). Human APP cDNA harboring the Swedish mutation (K670N/671L) and human Tau harboring the P301L mutation are expressed in the PS1M146V "knock-in" mice. Age dependent AB and Tau pathology occurs around 6 months of age in 3xTgAD mice (211). Cognitive impairment in 3xTgAD mice emerges as a long-term retention deficit starting at 4–6 months of age and further develops in an age-dependent manner. There is a transient sex divergence in 3xTgAD pathology, such that female 3xTgAD mice exhibit enhanced cognitive deficits compared with age-matched male 3xTgAD (211,212). *Therefore, we will utilize only female 3xTgAD mice for these studies.* We will use two age groups of 3xTgAD mice to determine the contribution of HIF1α during TI on the initiation and exacerbation of AD-pathology. *Group 1 mice will begin the dietary restriction at 2 months of age* since nominal AD-pathologies in particular Aβ have been described (210,211,213,214). Previous studies have established that TI can promote Aβ plaques in the hippocampus, cortex, and thalamus in 2-month-old Tg19959 transgenic mice (1). Therefore, this age group will allow us to determine if HIF1α inhibition can delay the onset of Aβ plaque formation as a consequence of TI. *Group 2 mice will begin the dietary restriction at 6 months of age* since detectable Aβ plaque and tau phosphorylation occurs at 6 months of age in 3xTgAD mice and progresses in an age dependent manner (211). TI treatment has been shown to enhance Aβ plaque deposition and tau phosphorylation in the cortex and hippocampus of 5-month-old APPswe/PS1dE9 transgenic mice (2). Therefore, this age group will allow us to determine the impact of HIF1α inhibition to minimize TI induced progression of Aβ deposition and NFT's.

Our experimental approach will be to utilize YC1 [3-(5'-hydroxymethyl-2'-furyl)-1-benzylindazole] as a prototypical HIF1α inhibitor. Our published *in vitro* discoveries and preliminary results clearly establish that YC1 can minimize HIF1α activation during TI, which is consistent with mechanistic evidence establishing that YC1 represses expression and inhibits the transactivation of HIF1α (35,215,216). YC1 has also been previously evaluated *in vivo* in ischemic stroke models and for improving cognitive function in aging rats, further justifying the use of YC1 for these studies (217-221). Age matched female mice will be randomized into the following treatment groups: (1) control diet (AIN-76A) (CTL); (2) Graded levels of TI; (3) CTL+YC1 – adjusted for time frame of different TI diets; (4) Graded levels of TI + YCI. Mice will be pair fed to ensure isocaloric intake for each group. Mice will be administered YC1 at a dose of 1mg/kg/day via food intake. This dose was selected based on

daily administration providing beneficial results in rodents on memory function (217). Administration of YC1 IP to mice as high as 5mg/kg/day for 28 days was safe and effective in preventing the development of hypoxia induced pulmonary arterial hypertension (222). YC1 dosing via food intake was selected as it provides a more suitable way for long term administration by avoiding potential aversion to water-based dosing and minimizing pain/distress from daily injections or gavage. The volume of food consumed per day will be calculated per mouse. The volume of food provided and amount of thiamine or YC1 supplemented will be based on the cohort with the lowest amount of food consumed to ensure isocaloric intake and consistent/appropriate quantity of thiamine and dosing of YC1. Mice will begin YC1 treatment upon starting TI diets. Mice will be fed diets for up to 3 months with mice subjected to assessments described below every 2-4 weeks depending on the thiamine diet level. The length of time was chosen to provide a sufficient interval for responses in the mild/moderate TI groups, which can take longer than the expected 4/5-week onset with TI (0 T) (2,174-177). Assessments every 2 weeks with the TI (0 T) group and 1 month for the moderate/mild TI groups will provide a temporal relationship into the effectiveness of HIF1α inhibition to minimize/delay TI induced AD pathology. With an anticipated 2-fold change (based on the observed 2-fold reduction of C99 Fig 6C), sigma of 0.4, and power of 0.8, we calculate using a minimum of n=4 female mice per diet group/time point.

2.1. Quantification of Thiamine/Thiamine Phosphorylates, YC1, and Thiamine enzyme activity: We will utilize the same approach to quantify T/TMP/TDP and thiamine dependent enzyme activity as stated in aim 1.2 to establish thiamine status changes. Evidence using YC1 to limit neurological damage strongly suggests YC1 reaches the brain *in vivo* (217-221). Our collaborator, Dr. Michael Bartlett will utilize his expertise and experience to develop an analytical assay for detection of YC1 in blood and whole brain homogenate to confirm.

2.2. Determination of HIF1α activity: Mechanistically, YC1 has been shown to inhibit HIF1α expression and reduce transcriptional activity (223). To determine the change in functional activity of HIF1α with TI and YC1 administration, we will utilize an ELISA-based HIF1α transcription factor assay. Our lab has previously used this approach to demonstrate HIF1α activity (203). The more functional HIF1α present, the greater HIF1α binding to the R-CGTG HIF1α consensus sequence bound to the plate surface. We anticipate a decrease in the absorbance reading (less activated HIF1α) in mice receiving YC1. To validate these findings, we will perform WB for HIF1α on brain homogenate using established methods.

2.3. Expression and activity of HIF1α regulated BACE1: Total BACE activity is increased in AD and the mRNA of BACE1, the predominant brain form, is elevated in AD brains (224,225). Both hypoxic stress via HIF1α and TI increase BACE1 expression, activity, and APP processing (1,3,43,46). The changes in BACE1 expression will be assessed using qRTPCR and WB using methods well established in our laboratory. Total BACE1 activity will be determined by a fluorometric assay as shown in Fig.6A. To validate our findings for BACE1 expression and activity we will also quantify cleavage of APP by BACE β-CTF (C99) by WB (Fig.6B).

2.4. Quantification of Aβ deposition, Tau phosphorylation, and neurofibrillary tangle (NFT) formation: The amyloid hypothesis states that Aβ peptides lie upstream of the pathological events occurring in AD, including neurofibrillary tangle (NFT) formation, synaptic dysfunction, and neuronal death (210,226,227). Aβ peptides are cleaved from a plasma membrane spanning protein known as amyloid precursor protein (APP) (228). Both $A\beta_{40}$ and $A\beta_{42}$ peptides have been shown to accumulate in mouse models of TI and after hypoxia induced induction of HIF1α (1,3,43,47). We will quantify changes in Aβ peptides by WB, ELISA, and IHC from brain sample homogenates using established methodology (204,205). Cleavage of Tau by caspases 3/7 can lead to Tau aggregation and phosphorylation (229,230). Our published results demonstrate that TI increased caspase 3 activity in astrocytes that was attenuated by the HIF1α inhibitor YC1 (35). We will measure the extent of Tau phosphorylation by WB and IHC and caspase activity (aim 1.7) as an indicator for progressive AD pathology. Since NFT formation lies downstream of Aβ, NFT formation will be expected to occur in our group 2 (6 month) animals that could be associated with progressive cognitive impairment in our behavioral assessments. Tau phosphorylation and NFTs will be measured using IHC and WB using established methodology (204,205).

2.5. Neurotoxicity markers: Synaptic dysfunction is a likely contributing factor causing progressive cognitive deficits in 3xTgAD mice. There is a marked increase in synaptic dysfunction with increasing age in these mice coincident with a significant decline of the presynaptic vesicle glycoprotein synaptophysin (210). We will perform WB to quantify synaptophysin levels in brain tissues using established methodology (205). We anticipate that YC1 treatment during TI will preserve synaptic function indicated by an increase in synaptophysin levels. For cell specific evaluations we will probe for NeuN and GFAP immunoreactivity, for neurons and astrocytes, respectively. Furthermore, we will probe for Iba1 as a marker for microglia cell proliferation and an indicator of neuroinflammation. Since astrogliosis and increase in microglia are associated in mouse models of AD, we anticipate that YC1 during TI will exhibit attenuated GFAP and Iba1 reactivity (210). Literature suggests that YC1

treatment reduces reactive astrocyte formation and neuroinflammation within ischemic models (219,231). We expect to preserve NeuN levels with YC1 treatment during TI that would indicate reduced neuronal death.

2.6. Behavioral assessment: As noted in Aim 1.6, cognitive/memory deficits will be assessed using the Barnes Maze and Novel Object Recognition tests to be performed using established methods by our co-investigator, Dr. Nikolay Filipov (201,202).

Anticipated results, potential pitfalls, and alternative approaches: The objective for this aim is to establish HIF1α activation during TI as an initiator and progressive influence for AD neuropathology. We expect that TI diet will reduce T/TDP levels, reduce TDP enzyme activity, and YC1 treatment in combination with TI will inhibit/attenuate HIF1α stabilization and activity (aim 2.1+2.2). We expect that induction and activity of BACE1 will be reduced by HIF1α inhibition during TI (aim 2.3). Lastly, in both age groups we expect delayed onset and reductions in Aβ deposition, NFT formation, preservation of neurons and synapses, and minimization of reactive astrocyte formation in TI+YC1 treatment compared with only TI treated 3xTg-AD mice (aim 2.4+2.5). We anticipate that mice on TI diets receiving YC1 will have a delayed onset (Group 1 mice) and diminished progression (Group 2 mice) in cognitive/memory deficits (aim 2.6).

The use of YC1 to inhibit HIF1α and delay/reduce AD-pathology during TI could be invalidated when objectively tested. Although YC1 is a well-established HIF1α inhibitor, it can also function to activate the NO-sGC-cGMP pathway (232). The dual activities of YC1 are concentration-dependent with low conc's of YC1 capable of inhibiting HIF1α activity and higher conc's required for cGMP elevation (233). Mice dosed with 30 mg/kg YC1 demonstrated activity primarily via HIF1α inhibition (233). Appropriate controls (YC1 alone), low dose (1mg/kg/day), and measurement of HIF1α expression/activity will provide us with an ability to confirm target specificity of YC1 for HIF1α inhibition to test our hypothesis. Since activation of sGC promotes an increase in cGMP, we will also quantify changes in cGMP (cGMP assay kit – Abcam) in our brain samples to evaluate off target activity during our treatments (234,235). Intriguingly, activation of the NO-sGC-cGMP pathway by YC1 may play a role in improving learning and memory functions in aged rats (217,236). By affecting both sGC and HIF1α, YC1 maybe a promising dual target approach that should be contemplated. In the unlikely event YC1 dosing produces negligible HIF1α inhibition and/or significant off target activity, we would adjust the dose of YC1, or we could use the selective HIF1α inhibitor, PX-478 (237-239). Metabolic disruption by TI also promotes oxidative stress (1,21,168,240). In addition to being involved in AD-neuropathology, oxidative stress can induce the activation of HIF1α (241-243). The neurotoxicity mediated by oxidative stress and HIF1α may be synergistic during TI and a single targeted approach using YC1 may be unable to significantly delay or reduce AD pathology markers evaluated in this aim. To this end, we could us an approach combining TI with the antioxidant, MitoQ. MitoQ has been established to delay disease initiation and progression in 3xTgAD mice (204,205).

Aim 3: Establish the molecular phenotype associated with graded nutritional thiamine insufficiency

Introduction: The cellular and molecular pathways regulated by HIF1α that mediate survival and death are multifaceted. Pro-death pathways include genes involved in oxidative stress, inflammation, apoptosis, iron/calcium homeostasis, autophagy, and excitotoxicity (39,41,244). Pro-survival involves angiogenesis, erythropoiesis, metabolism, and nutrient transport (39,41,244). What drives pro-survival and/or pro-death signatures is still unresolved but has been contextually associated with the duration, severity, cell type, and age. (49,109-111,125,132,245-249). Our *in vitro* work has clearly established select HIF1α regulated genes that mediate TI induced neuropathology. Recently, non-canonical gene expression regulated by HIF1α was uncovered in a cell type specific manner using RNA-seq (131). Unfortunately, cell type specific targets and the temporal onset of prosurvival and prodeath HIF1α genes during graded TI remain undiscovered. Therefore, *the objective for this aim* is to determine the temporal onset and contextual relationship of HIF1α regulated gene expression during graded nutritional TI. *Our working hypothesis* is that chronic TI predominantly activates HIF1α directed neuropathological pathways in a regional, cell dependent and temporal manner. *Our approach* will be to use RiboTag technology for cell specific whole transcriptome sequencing to establish the molecular phenotype during TI. *We*

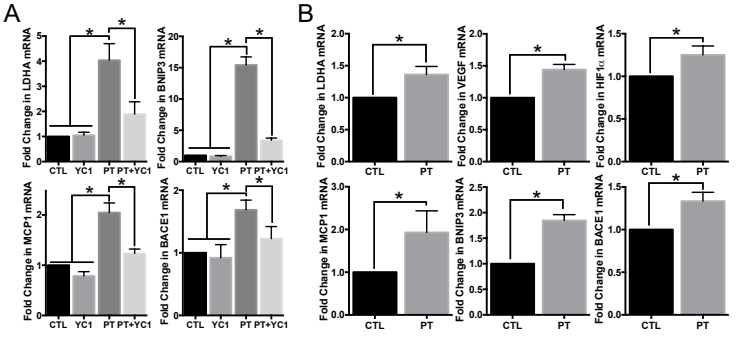

Figure 7: TI induces HIF1α regulated genes expression in (A) Mouse hippocampal HT22 cells treated with either 3μM thiamine containing media (CTL), 10μM YC1, 10μM PT, or both YC1 and PT for 3 days (B) Whole brain tissue from 11-mth old C57BL/6 mice injected IP daily for 7 days with 10mg/kg PT or with vehicle (CTL). Real time-PCR analysis of mean mRNA expression for N=3 independent expts. Data are normalized to Actin and relative to control using the $2^{-\Delta\Delta Ct}$ method. (★) Represents a statistically significant difference of $p<0.05$ based on the results of a one-way ANOVA with Tukey's post-hoc test for (A) and T-test for (B).

expect that chronic TI will initiate HIF1α regulated neuropathological gene expression in sensitive brain regions and that an unbiased analysis will uncover novel cell specific signatures in response to chronic TI.

Justification, Feasibility, and Preliminary Data: To date no comprehensive bioinformatic study has delineated gene expression changes selectively within cell type or extent of TI. Using an Affymetrix GeneChip approach comparing ~16,000 transcripts, TI up-regulated genes associated with metabolism, inflammation, and cell death (157). ***Intriguingly, the authors noted significant overlap of gene expression patterns to those observed in focal ischemia*** (157). A proteomic study also noted changes in metabolic gene expression following TI (250). However, these studies did not provide an unbiased gene expression comparison within two major cell types impacted by TI, astrocytes and neurons.

Our published discoveries are the first to demonstrate transcription of both pro-survival (LDHA, GLUT1, VEGF) and pro-apoptotic/inflammatory (MCP1, BNIP3, NIX, NOXA) HIF1α target genes within TI treated astrocytes (34,35). Up-regulation of VEGF may explain the clinical observation of high circulating VEGF and cerebral blood flow hyperperfusion (251,252). The activation of HIF1α during TI may explain the increase in LDHA expression and lactic acidosis (136,253). TI in HT22 cells significantly induced transcription of HIF1α regulated genes LDHA, BACE1, MCP1, and BNIP3 that was attenuated with the HIF1α inhibitor YC1 (Fig.7A). Transcription of VEGF, BNIP3, LDHA, BACE1, MCP1 were also significantly upregulated in whole brain samples from 11-mth old C57BL/6 TI mouse model compared to vehicle treated age matched controls (Fig.7B). Although these results demonstrate expression of survival, inflammatory, and apoptotic genes this may be due to a biased assessment of whole brain, *in vitro* models with lack of cell-to-cell relationships and a need for temporal and thiamine status factors. Therefore, the premise to determine the molecular phenotype in a contextual manner is impactful and necessary to dissect the chronic implications of TI stress and HIF1α responses.

Research Design: To isolate astrocyte or neuron enriched mRNA we will utilize RiboTag mice (B6J.129(Cg)-Rpl22$^{tm1.1Psam}$/SjJ – Jackson Lab) crossed with either GFAP-Cre (B6.Cg-Tg(Gfap-cre)77.6Mvs/2 – Jackson Lab) or Syn1-Cre (B6.Cg-Tg(Syn1-cre)671Jxm/J – Jackson Lab), respectively. AD and other dementias occur greater in elderly women than males, suggesting sex differences in the onset of neuropathology (172). Recently, lower TDP levels were found in a cohort of female subjects compared to males (16). To evaluate any sex related differences in HIF1α regulated genes in response to TI, both male and female homozygously floxed mice will be included and analyzed collectively and separately. Age related differences in the responses to TI have been reported, with the greatest response occurring in older mice than in young mice (169-171). Thus, mice at 15 mos. (~50 human yrs.) of age will be used (173). With an anticipated 2-fold change (based on the minimum change in gene expression– Fig.7), sigma of 0.4, and power of 0.8, we calculate using a minimum of n=4 male and n=4 female mice per diet group/time point. *Feeding/time points*: Following a conditioning period to normal control liquid diet (2 weeks), mice will be randomly divided into each dietary restriction group. Mice will be fed graded thiamine diets for up to 3 mths with mice subjected to assessments depending on the thiamine diet level. Assessments every 2 weeks with the TI (0 T) group and every month for the moderate/mild and CTL group will provide a temporal relationship for the onset of HIF1α activation based on thiamine intake levels. The length of time was chosen to provide a sufficient interval for responses in the mild/moderate TI groups, which can exceed the expected 4/5-week onset with TI (0 T) (174-177). We will iteratively adjust the feeding time frame and assessment interval based on the outcomes.

3.1. Physical assessment and Thiamine status: As described in aim 1.1 and 1.2 we will assess for ataxia and LORR at each time point. The intent of this evaluation will be to quantify the onset and severity of the physical signs of TI and to correlate with our transcriptome analysis. Our proposed transcriptomic analysis will be able to establish expression differences in PDH, α-KGDH, and TKT and changes in activity with direct measurements of T/TMP/TDP will define changes in thiamine status within our thiamine restriction groups.

3.2. Transcriptome changes using RNA-Seq: Stabilization of HIF1α leads to activation and induction of a wide array of gene expression (39). We will use a transcriptome approach to globally assess the transcriptional activity of HIF1α induced during TI. Varying time point assessments during thiamine dietary restriction presents an opportunity to ascertain the temporal influence of progressive TI to induce HIF1α regulated genes, and to establish any clustering and gene expression relationships that may reflect TI neuropathology as a whole.

3.2.1. Regional isolation: Gene expression can vary in different brain regions and within the same cell types (254,255). TI is well established to produce substantial neurotoxicity in the thalamic region (256,257). Additional regions such as the hippocampus and cortex are also impacted with long term and severe TI (258-260). Therefore, isolating thalamus, hippocampus, and cerebral cortex tissue will be utilized to compare transcriptome differences regarding TI induced HIF1α transcriptional activity. Excised mouse brain will be dissected using the mouse brain atlas (http://www.brain-map.org) to assist in brain region identification.

3.2.2. Affinity tag and RNA isolation: Hemagglutinin (HA) affinity tagged ribosomes will be isolated from homogenized tissue using the immunoprecipitation (IP) kit - Dynabeads-protein G (Invitrogen) as per Mfr. protocol. For each isolated brain region, a portion of the homogenate will be retained as input sample and used for T/TMP/TDP quantitation and enrichment analysis (see 1.2 and 1.3.4, respectively). RNA will be isolated using EZNA total RNA kit and the quality of the extracted RNA evaluated using the Bioanalyzer RNA 6000 Nanochip. Samples that have RNA integrity number greater than 8 will be used to build the RNA-Seq libraries.

3.2.3 RNA sequencing and analysis: RNA sequencing library construction, sequencing and data analysis will be performed at the Georgia Genomics and Bioinformatics Core (GGBC) lab in collaboration with Dr. Kaixiong Ye. RNA-seq libraries will be prepared using the Illumina compatible Kapa RNA HyperPrep kit following the Mfr. protocol. The libraries will be barcoded to allow multiplexing of samples in the same sequencing run. After assessing the quality of the libraries, they will be pooled at equimolar ratios and sequenced on the NextSeq 500 platform. The goal is to generate 25-30 million paired-end 75-bp reads per sample. Quality control of sequencing reads will be done with the Trim Galore tool, which streamlines quality assessment with FastQC and adaptor trimming with Cutadapt. Then the reads will be mapped to the mouse reference genome (mm10) using STAR (261,262). The read-mapping results will be used to perform the differential gene expression analysis using the statistical package edgeR (263,264). The results will be a list of significantly differentially expressed genes (FDR < 0.05) between samples. Pathway enrichment of differentially expressed genes will be evaluated using DAVID and GAGE (265,266). Gene expression differences in pathways of special interest (e.g., HIF pathway, thiamine homeostasis, etc) will be visualized with Pathview (267). We will validate expression changes of select genes of interest uncovered in our RNA-Seq results using Western blot and qRTPCR (268).

3.2.4. RiboTag validation: To ensure RiboTag astrocyte and neuronal pull-down fraction enrichment we will utilize qRTPCR. RNA from HA-IP samples and input sample will be converted to cDNA and qRTPCR performed and analyzed using established methods as stated in our previous publication (35). Samples will be evaluated for GFAP, NeuN, Iba1, and APC for astrocytes, neurons, microglia, and oligodendrocytes, respectively. The percent expression compared to the input sample will be determined to evaluate enrichment. We expect enrichment to be >95% for astrocyte and neuronal markers in the corresponding HA-IP samples and be less than 1% for all other cell type makers evaluated. Previous reports have demonstrated high degree of recombination in both astrocytes and neurons within RiboTag mice, therefore we anticipate similar (269,270).

Cells expressing either GFAP or SYN1 Cre recombinase will drive HA tagged ribosomal subunit production. To ensure widespread expression of HA-tagged ribosomes within our brain regions of interest (thalamus, cortex) we will utilize an immunofluorescence (IF) approach. Briefly, mice will be transcardially perfused with 4% PFA. Excised brain will be placed in 25% sucrose with 4% PFA solution, flash frozen, and stored at -80^{o}C. Brains will be sagittaly cut down the midline and 20μm thick slices will be prepared using a cryostat and processed for IF staining. primary antibodies targeting HA, SYN1, and GFAP will be used. Marker fluorescence will be analyzed with a Nikon Microscope Eclipse Ti as previously performed (35). For quantification, the fluorescence intensity of at least three random fields from 5 serial sections for each brain will be determined using ImageJ software. Analysis in the Z-plane will be done to ensure cells expressing different markers are not located on top of one another will be used to compare fluorescent intensity.

Anticipated results, potential pitfalls, and alternative approaches: The objective of this aim is to determine the temporal impact of graded TI stress to stimulate HIF1α transcriptional activity within neurons and astrocytes We expect mice fed a thiamine restricted diet will produce progressive neurological symptoms and reduced T/TMP/TDP and TDP dependent enzyme activity (aim 3.1). Since early-stage gene expression mediated by HIF1α involves adaptive gene expression our expectation is that the early phase response attempts to overcome mild/moderate TI stress. We also expect that with continuous TI stress, activation of pro-death pathways will predominate and be rank ordered with the degree of thiamine status (aim 3.2).

Although our preliminary data strongly supports a role for TI to promote HIF1α transcriptional activity *in vitro*, there is a remote possibility that it could be invalidated when objectively tested *in vivo* using senescent mice. HIF1α activation is predominantly regulated through HIF-PHD2, however pyruvate accumulation can reduce activity of all three PHD isoforms (89,271,272). Pan HIF-PHD inhibition could result in additional transcriptional factor activation regulated by other HIF-PHDs, including but not limited to the stress transcription factor ATF4 and NFkβ (100-103). We would expect that our whole transcriptome sequencing would be capable of establishing known gene expression from these transcription factors. To establish transcriptional factor gene selectivity, we would utilize a CHIP-seq approach for HIF1α pull down.

Timeline: Since breeding of our proposed LOXP-Cre mice for aim 1 will take multiple generations to provide sufficient animals, we expect to initiate work in year 1 and complete by year 3. We plan to conduct research on aim 2 between year 2 and 4. Finally, we will start work on aim 3 in year 2 and complete by end of year 5.